# NEW AIRBORNE CLOUD EXTINCTION PROBE

Alexei Korolev
*Environment Canada, Toronto Canada*

## 1. INTRODUCTION

The extinction coefficient is an important parameter in characterizing bulk microphysics properties of clouds. Knowledge of the extinction coefficient is of crucial importance for radiation transfer calculations in weather predictions and climate models, as well as validation of remote sensing and satellite retrievals (e.g. Barker et al. 2008).

Early attempts to use airborne extinctiometers for measurements of visibility in clouds go back to works of Kampe (1950) and Weickmann and Kampe (1953). The first airborne extinctiometer utilized the transmissiometric method. It consisted of incandescent lamp, collimator and a photocell for measuring the light intensity. The source of light separated by a few meters from the photocell were mounted on the wing. Zabrodsky (1957) built an airborne a double pass transmissiometer where light traveled to a retroreflector and back, and then it was measured by a photodetector. Nevzorov and Shugaev (1972, 1974) built an advanced version of this transmissiometer with improved stability and high sensitivity. This was a successful design which allowed for the collection of a large data set on the extinction coefficient in different types of clouds (Kosarev et al, 1976; Korolev et al. 2001). King and Handsworth (1979) built a single pass transmissiometer with an ultraviolet source of light generated by a germicidal lamp. Zmarzly and Lawson (2000) designed a multi-pass and multi-wavelength Cloud Extinctiometer. Gerber et al (2000) built a Cloud Integrated Nephelometer where the extinction coefficient was calculated from an arrangement of four Lambertian sensors, two of which had a cosine masks.

*Author's address*: Alexei Korolev, Environment Canada, 4905 Dufferin Street, Toronto, Ontario, M3H5T4 Canada, e-mail: alexei.korolev@ec.gc.ca

In many studies the extinction coefficient of clouds was estimated from composite size distributions measured by several cloud spectrometers. Earlier measurements (Korolev et al. 1999) showed a good agreement between the extinction coefficient measured by a cloud transmissiometer and that derived from the PMS FSSP droplet size spectra. However calculations of the extinction coefficient from particle size distributions in ice and mixed phase clouds is subject to potentially large errors due to uncertainties related to the size-to-area conversion technique, shattering issues and limited accuracy in measurements of concentration and sizes of ice particles smaller than approximately 100$\mu$m.

Despite great significance of the extinction coefficient on our knowledge of the radiation transfer in clouds and the Earth's climate in general, probes that are capable of direct measurements of the extinction coefficient have not become a part of conventional airborne microphysical instrumentation. The effort to fill this gap has been undertaken by Cloud Physics Research and the Severe Weather Section of Environment Canada. This paper presents a description of the newly designed Airborne Cloud Extinction Probe. As well, some of the airborne measurement results of the extinction coefficient of clouds are discussed.

## 2. DESCRIPTION OF THE EXTINCTION PROBE

The Cloud Extinction probe utilizes the transmissiometric method. The principle of operation is based on the measurements of the attenuation of visible light between the emitter and receiver. This method enables the calculation of the extinction coefficient from first principles based on the Beer-Bouguer law. The Extinction Probe consists of an optical unit that combines a transmitter and receiver as well as a retroreflector.

Figure 1 shows a general schematic of the optical unit. A collimated light beam is generated by an optical system consisting from the superbright LED with the wavelength $\lambda$=0.635$\mu$m (1), diffuser (2), condenser (3), pinhole (4), and objective (5). The beam travels from the optical unit to the retroreflector (6), and then returns the same distance back to the optical unit. Then after passing though the objective and beam-splitter (7) its intensity is measured by a photodetector (8). The optical chopper (9) modulates the light beam and controls turning on and off the LED with the help of the optocouple (10). The optical chopper consists of a sequence of holes, dark areas and mirrors glued on its surface. During the first half of the period when the hole is opened, the LED is on, and the photodetector measures the intensity of transmitted light plus the background intensity ($I_{tot}$). During the second half of the period, when the hole is opened, the LED is off, and the photodetector measures the intensity of the background light ($I_{bkg}$). During the first half of the period, when the hole is closed, the LED is on, and the light is reflected from the mirrored surface. After passing though a beam-splitter the reflected light is measured by the photodetector ($I_{norm}$). This signal characterizes the intensity of the LED, and is used to normalize all other measured signals. During the second half of the period, when the chopper hole is closed, the LED is on and the beam hits the blackened surface of the chopper. In this case, the photodetector measures the signal ($I_{int}$) related to the light scattered inside the optical unit due to reflection from the optical surfaces and the different parts inside the probe's housing. The advantage of such a scheme is that it allows measurements of the intensities of the LED, background and attenuated light with the same photodetector. Utilizing of the above scheme minimizes the effect of changes of the photodetector sensitivity during flight (e.g. caused by temperature drift) on the measurements of the extinction coefficient.

The optical scheme was designed to produce a highly uniform collimated beam (Fig,2). The inhomogeneity of the light intensity across the beam does not exceed 1%. This minimizes the effect of vibration and mutual motion the optical unit and retroreflector with respect to each other during the flight operation. A similar approach has been used by Nevzorov and Shugaev (1974). The size of the retroreflector was chosen so that its

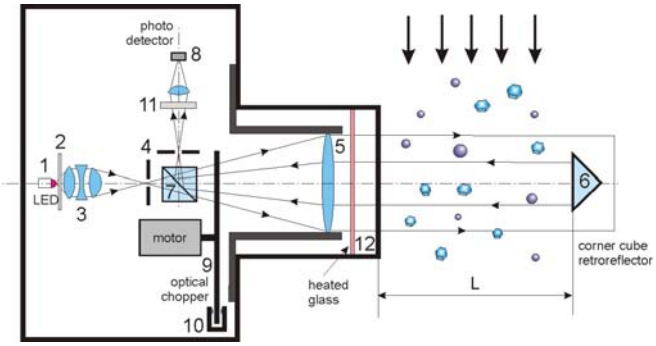


**Figure 1.** Schematic diagram of the Cloud Extinction Probe: (1) LED 0,635$\mu$m; (2) diffuser; (3) condenser; (4) pinhole; (5) objective; (6) cone cube retroreflector; (7) beamsplitter; (8) photodetector; (9) optical chopper; (10) optocouple; (11) filter; (12) front heated glass.

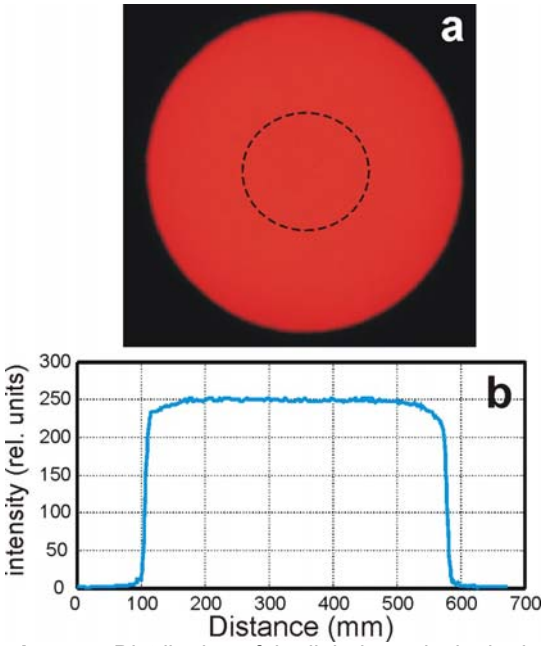


**Figure 2.** Distribution of the light intensity in the beam in the Cloud Extinction Probe. (a) beam cross-section. The dashed lines show the relative size of the retroreflector; (b) distribution of the intensity along the beam diameter

displacement from the center of the beam in each direction at the distance of approximately 1cm does not affect the output signal. The dashed lines in the center of the beam cross-section in Fig. 2a show the relative size of the retroreflector. During the flight the retroreflector always stayed inside the beam within the light intensity homogeneous area, whereas the reflected beam always stayed within the objective. This provides a stable output signal non-sensitive to the aircraft vibration.

The Extinction Probe was designed to operate in all weather conditions. The optics of the probe are well heated to prevent fogging, on impact with liquid droplets and during rapid aircraft descent at vertical speed higher 5m/s. The environment inside the optical unit is temperature controlled, so that the instrument can operate at air temperatures as low as -60°C. Based on the flight tests described in section 3, the threshold sensitivity of the probe was found to be approximately 0.2 $km^{-1}$. The upper limit of the measured extinction coefficient is estimated to be no less than 200 $km^{-1}$. The picture of the Extinction Probe is presented in Fig.3.

The Cloud Extinction Probe was installed on the National Research Council (NRC) Convair 580. The optical unit was mounted inside the wing tip canister and the retroreflector inside a hemispherical cap at the rear side of a PMS probe canister (Fig.4). The distance between the optical unit and the retroreflector was $L$=2.35m.


**Figure 3.** Cloud Extinction Probe: optical unit (top); control box (bottom); retroreflector (right).

The sample area of the probe is defined by the length of the beam ($L$) and the diameter of the reflector ($d$=25mm) and is calculated as $S=Ld$. For the installation on the Convair-580 $S\approx0.06m^2$. At a typical airspeed of 100m/s, the corresponding cloud volume sampling rate is approximately $6m^3/s$. Assuming a decent sensitivity, the above sampling rate allows measurements of a statistically significant extinction coefficient of ice particles with concentration few per cubic meter.

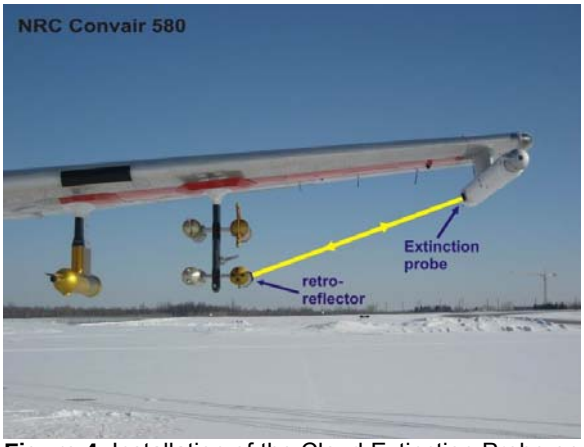


**Figure 4.** Installation of the Cloud Extinction Probe on the NRC Convair 580. The yellow line indicates the position of the beam under the wing.

## 3. CALCULATION OF THE EXTINCTION COEFFICIENT

The extinction coefficient measured by the Extinction Probe was calculated based on the Beer-Bouguer law as

$$\beta_{CEP} = -\frac{1}{2L}\ln\frac{I}{I_0} \qquad (1)$$

Here $I$ and $I_0$ are the output signals which characterize the radiant fluxes transmitted in clouds and in clear sky, respectively. The intensity of the attenuated signal was calculated as $I=I_{tot}-I_{bkg}-I_{int}$; $I_0$ was determined the same as $I$ but in a cloud free atmosphere. The signals $I_{tot}$, $I_{bkg}$ and $I_{int}$ were normalized on the current values of $I_{norm}$.

The Extinction Probe provides measurements of the extinction coefficient in any type of clouds regardless their phase composition, i.e. liquid, ice and mixed phase. Since there are no calibrating

standards for the attenuation of light by dispersed media, we attempted to compare the extinction coefficient measured by the Extinction Probe with that deduced from the PMS Forward Scattering Spectrometer Probe (FSSP) cloud droplet spectra in liquid clouds and from the PMS Optical Array Probes (OAP) 2DC and 2DP particle images in ice clouds.

In liquid clouds, the extinction coefficient was calculated from the FSSP droplet size distribution measured in fifteen size bins.

$$\beta_{FSSP} = \frac{\pi Q}{4}\sum_{j=1}^{15} n_j D_j^2 \qquad (2)$$

Here $n_i$, $D_i$ are the concentration and diameter of droplets in the FSSP *i*-th size bin; *Q* is the extinction efficiency. Since the size of the FSSP measured droplets $D>>\lambda$, then to a good accuracy it can be assumed Q ≈ 2.

In ice clouds the extinction coefficient was calculated from the OAP imagery. Optical Array Probes provide shadowgraphs of cloud particles, which pass though the sample area of the probe (Fig.5a). In general, the OAP can be considered as an extinctiometer, which instead of measuring of the attenuation of light integrated over the whole beam, measures local attenuation associated with the discrete binary images with the shadow areas $A_j$ (Fig.5b). Therefore, the extinction coefficient can be calculated through the integration of the area shadowed by all particles $\sum A_j$ as,

$$\beta_{OAP} = \frac{Q}{LA_0}\sum_j A_j \qquad (3)$$

Here *L* is the distance between the OAP arms (Fig. 5b); $A_0$ is the total area covered by the probe's laser beam having the width *W* and moving at speed *U* during time $\Delta t$, i.e. $A_0=WU\Delta t$. Substituting this expression into Eq.3 yields

$$\beta_{OAP} = \frac{Q}{LWU\Delta t}\sum_j A_j \qquad (4)$$

In this approach the transmittance $T=I/I_0$ in Eq.1 is approximated by the ratio $\sum A_j / A_0$, i.e. $I/I_0 \cong \sum A_j / A_0$.

The direct area calculation (DAC) technique of estimation of the extinction coefficient is based on the following assumptions regarding the OAP imagery: (1) the depth-of-field and the sample area width do not depend on the particle size, i.e. the sample area of the probe stays constant for all particles; (2) the shadow images represent geometrical shadows of cloud particles and the diffraction effects are neglected.

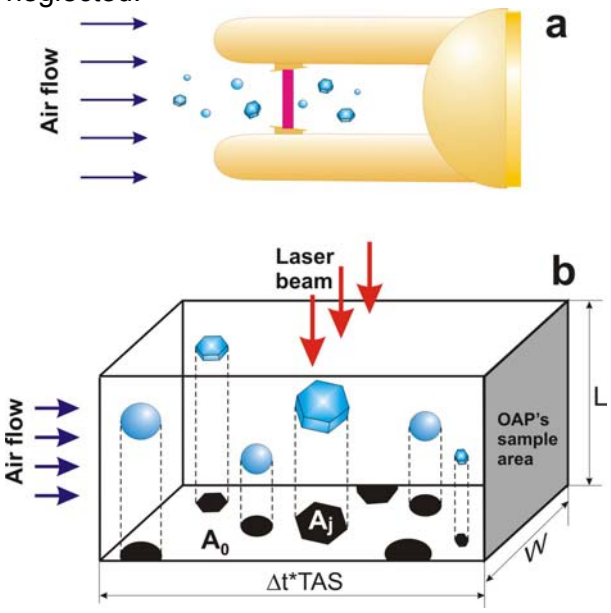


**Figure 5.** Conceptual diagram of calculation of the extinction coefficient from the OAP-2D imagery.

The assumption (1) is satisfied for particles with *D* ≥ 125μm for OAP-2DC and for particles with *D* ≥ 400μm for OAP-2DP, i.e. when the depth-of-field for these particles is larger than the distance between the arms. Korolev et al (1998) showed that the projected image area experiences several oscillations, when a particle moves from the object plane to the edge of the depth-of-field. The effect of the particle distance on the projected area decreases with the increase of particle size. In other words the DAC technique is expected to work better for larger particles than for the small ones. It should be mentioned that calculation of the extinction coefficient from OAP-2DP/2DP imagery in ice clouds with large concentration of ice particles

($D$<100μm) may result in significant underestimation of the extinction coefficient.

The DAC method gives more accurate estimation of the extinction coefficient, as compared to the alternative method based on the size-to-area conversion (STAC) $A=aD^b$. The sources inaccuracy for the size-to-area conversion method are related to the uncertainty in the coefficients $a$ and $b$ for different particle habits. The size-to-area conversion also cannot be applied to partial images, which significantly limits the use of STAC method for particles with $D>W$.

## 4. RESULTS OF MEASUREMENTS

In this section we demonstrate the performance of the Cloud Extinction Probe in liquid, ice and mixed phase clouds and compare the results of its measurements with the extinction coefficient calculated from the size distribution measured by the PMS FSSP, OAP-2DC and 2DP.

*Liquid clouds*

Figure 6 shows the results of the measurements of the extinction coefficient during flights through strato-stratocumulus. The high frequency of cycling of the Rosemount Ice Detector (RICE) signal (Fig.6c) indicates that the cloud contains supercooled liquid water. As seen from Fig.6a the extinction coefficient measured by Extinction Probe and that calculated from the FSSP varied from approximately 20 to 120km$^{-1}$. The studied cloud layer also contained some ice particles. However, the estimations from the OAP-2DC/2DP imagery suggest that the extinction coefficient associated with ice is lower than 1km$^{-1}$ for the most of the cloud. This value is much less than the extinction coefficient associated with liquid. Therefore, this cloud layer can be considered as conditionally liquid and the effect of ice particles on the extinction coefficient measured by the Extinction Probe and FSSP can be neglected.

Figure 7 shows the scatter diagram with the comparisons between Extinction Probe and FSSP measurements of the extinction coefficient. As seen from Fig.7 in liquid clouds the extinction coefficients measured by the Extinction Probe and FSSP agree reasonably well with each other.

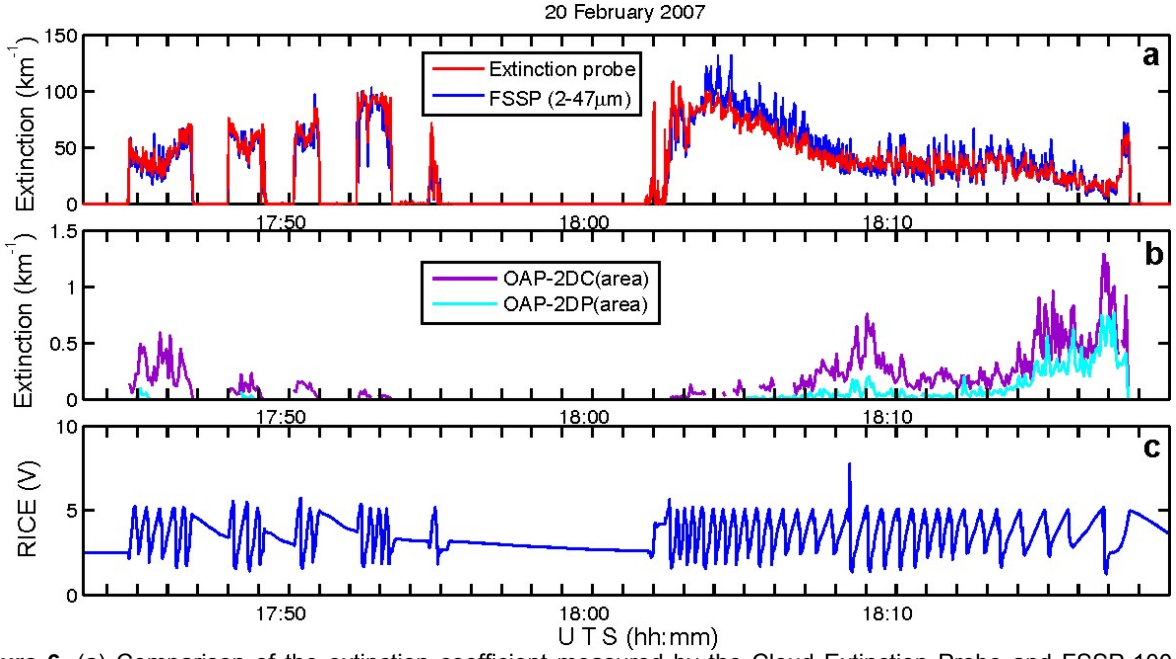


**Figure 6.** (a) Comparison of the extinction coefficient measured by the Cloud Extinction Probe and FSSP-100 (3-47μm), (b) Extinction coefficient deduced from the measurements of OAP-2DC and 2DP; (c) Rosemount Icing Detector signal. The oscillating RICE signal indicates on presence of supercooled liquid. Measurements were conducted in St-Sc, 1500<H<1800m; T=-10C, Southern Ontario.

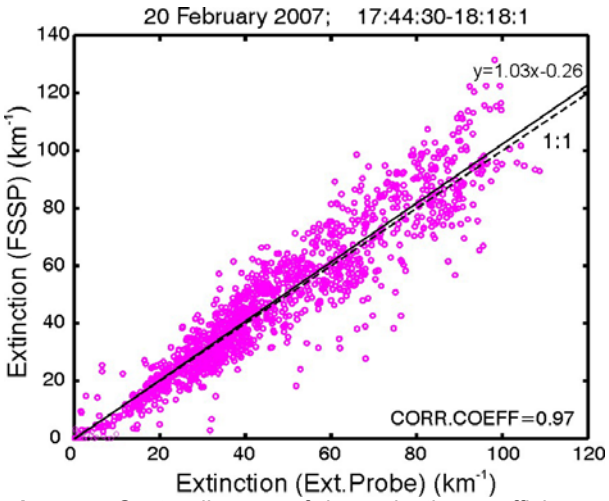


**Figure 7.** Scatterdiagram of the extinction coefficient measured by the Cloud Extinction Probe and that measured by FSSP-100 for the cloud segment shown in Fig.6a.

*Ice clouds*

Figure 8 shows spatial variations of the extinction coefficient during a flight beneath a precipitating altocumulus. The continuous decrease of the RICE signal in Fig.8b indicates on the absence of liquid along the flight line (Mazin et al. 2001), which helps identify this cloud as glaciated. The images measured by the OAP-2DC shown in Fig.9 suggests that most ice particles were spatial dendrites having irregular shape with maximum size varied from 6mm at the beginning of cloud and up to 10mm at the end.

The scatterdiagrams in Fig.10 show good agreement between the extinction coefficient measured by the Extinction Probe and that derived from the OAP-2DC/2DP. The OAP extinction coefficient was calculated using Eq.4. The agreement between the Extinction Probe and OAP suggests that the major input to the extinction coefficient is due to particles larger than approximately 200μm. This indicates absence of a high concentration of small ice particles in this cloud, which can noticeably affect the extinction coefficient.

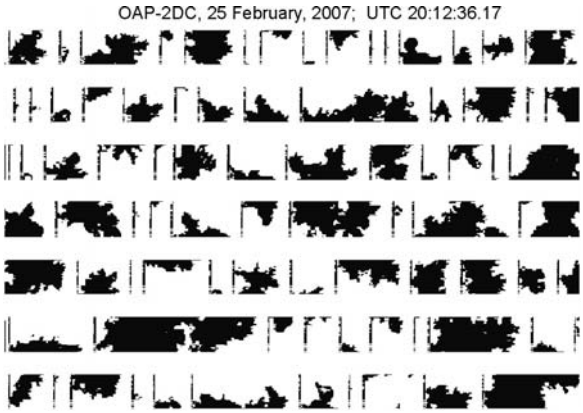


**Figure 9.** OAP-2DC imagery of ice particles from the cloud shown in Fig.8.

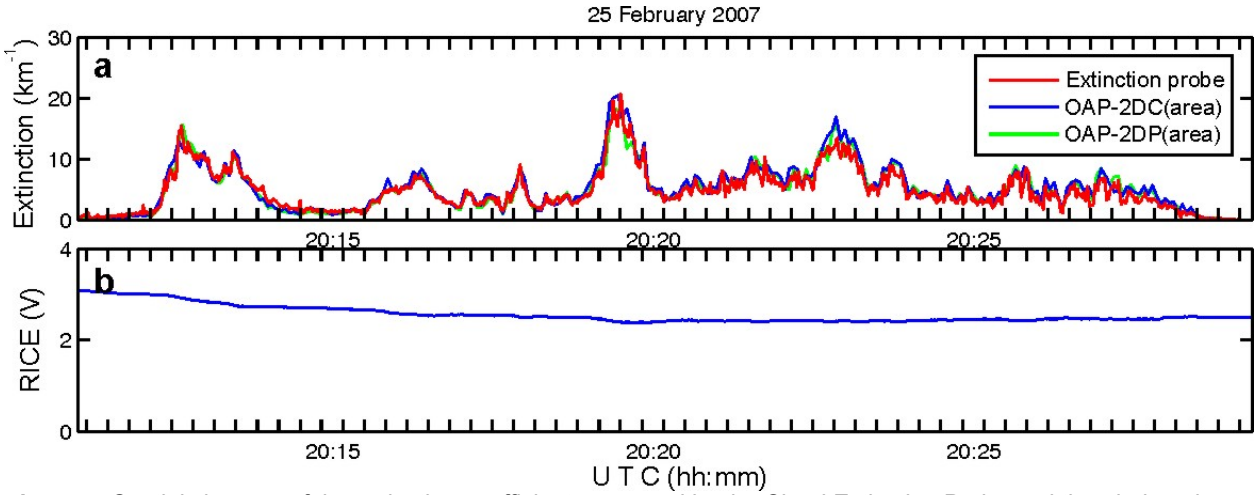


**Figure 8.** Spatial changes of the extinction coefficient measured by the Cloud Extinction Probe and that deduced from the cloud particle image areas measured by OAP-2DC and OAP-2DP (a). Rosemount Icing Cylinder signal (b) during traverse of precipitating region of altocumulus, 4500<H<5500m, -20<T<-15C, Southern Ontario.

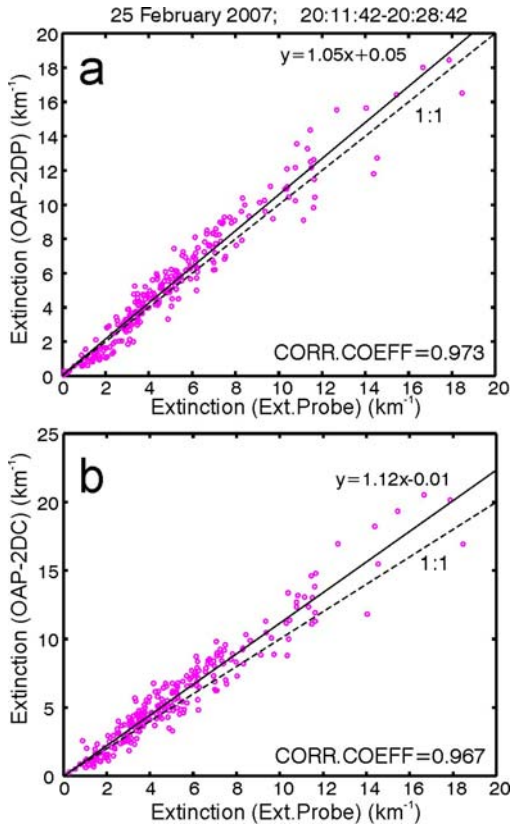


**Figure 10.** Scatterdiagram of the extinction coefficient measured by the Cloud Extinction Probe and that calculated from cloud particle images areas measured by OAP-2DC (a) and OAP-2DP (b) for the cloud segment shown in Fig.8.

*Mixed phase clouds*

Joint analysis of the extinction coefficient measured by the Extinction Probe and OAPs, in some cases allows for the separation of the extinction coefficients associated with liquid and ice in mixed phase clouds. Figure 11 shows a spatial variation of the extinction coefficient during descent through a precipitating stratocumulus. The airplane traversed through the topmost cloud layer, which was at 1500m at 13:48 (leftmost side of the Fig.11a) and then leveled flight at 1100m at 13:51. The cloud had liquid top with no ice particles. However, the ice particles began to appear at lower levels and then amount of ice increased during a horizontal flight from approximately 13:52 to 14:00. During the leveled flight, the Convair 580 traversed though three mixed phase zones highlighted in grey in Fig.11. The presence of liquid is indicated by the oscillations (1st zone) or gradual increase (2nd and 3rd zones) of the RICE signal. In mixed phase cloud regions, the extinction coefficient measured by the Extinction Probe is larger than that calculated from the OAPs. Since OAP-2DC is insensitive to cloud droplets with $D$<30μm, and assuming that cloud particles with $D$>50μm are all ice, this assumption allows for the estimation of the extinction coefficient of ice particles as $\beta_{ice} \approx \beta_{AOP}$. Therefore, the extinction coefficient for liquid droplets can be estimated as

$$\beta_{liq} = \beta_{CEP} - \beta_{OAP} \qquad (5)$$

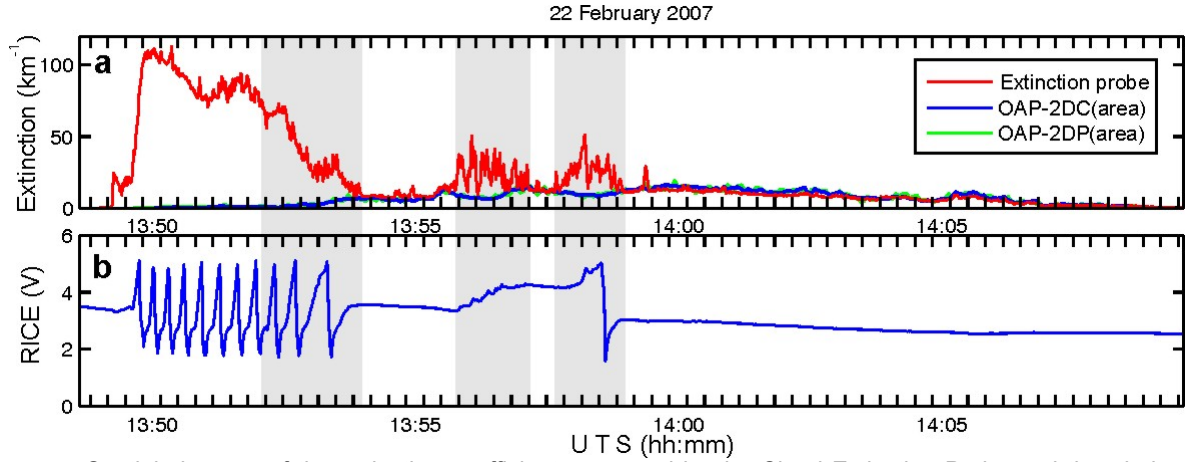


**Figure 11.** Spatial changes of the extinction coefficient measured by the Cloud Extinction Probe and that deduced from the cloud particle image areas measured by OAP-2DC and OAP-2DP (a) and the Rosemount Icing Cylinder signal (b) during traverse of stratocumulus, 1100m<$H$<1800m, -6<$T$<-2C, Southern Ontario. Highlighted grey areas indicate mixed phase cloud regions.

It should be noted that the above approach of separation of the extinction coefficient for liquid and ice can be applied only for mixed phase clouds with a relatively low concentration of small ice particles with $D$<50$\mu$m. Particles of this size are invisible to the OAP-2DC/2DP, and if such particles are present in significant numbers, $\beta_{ice}$ will be underestimated from $\beta_{AOP}$.

## 5. CONCLUSION

A new airborne Cloud Extinction Probe utilizing the transmissiometric technique has been designed by Environment Canada and tested on the NRC Convair 580 airplane. The Extinction Probe demonstrated the capability to measure the extinction coefficient in ice, liquid and mixed phase clouds. The threshold sensitivity is estimated at 0.2 $km^{-1}$. The extinction coefficient measured by the Extinction Probe agrees well with that calculated from the FSSP droplet spectra in liquid clouds and that deduced from the OAP-2DC/2DP images in ice clouds.

The advantages of the Extinction Probe are its large sample area (~60$cm^2$) and its measurements are practically not contaminated by shattered ice particles. Ice shattering and droplet splashing by sampling inlets is a serious problem for most optical cloud microphysical instruments. The Cloud Extinction Probe can be used to identify and characterize shattering and splashing efficiency of different cloud particle size spectrometers.

*Acknowledgements*: The author expresses gratitude to Vladimir Torgashev for his role in the mechanical design of the Cloud Extinction Probe. Special thanks to Rob Reed of Environment Canada for his support of the electronic functionality of the probe during the C3VP flight campaign, and to the NRC staff for the help for the installation of the Extinction Probe on the Convair 580.

## BIBLIOGRAPHY

Barker, H. W., A. V. Korolev, D. R. Hudak, J. W. Strapp, and K. B. Strawbridge A. 2008: Comparison between CloudSat and Aircraft Data for a Multi-layer, Mixed-Phase Cloud System during C3VP. *J. Geophys. Res.* (submitted)

Gerber, H., Y. Takano,T. J. Garrett and P. V. Hobbs, 2000: Nephelometer Measurements of the Asymmetry Parameter, Volume Extinction Coefficient, and Backscatter Ratio in Arctic Clouds. *J. Atmos. Sci.,* **57**, 3021-3034

Kampe, aufm, H.J., 1950: Visibility and Liquid Water in Clouds and in the Free Atmosphere. *J. Atmos. Sci.,* **7**, 54-57

King, W. D., and R. J. Handsworth, Total droplet concentration and average droplet sizes from simultaneous liquid water content and extinction measurements, *J. Appl. Meteorol.*, *18,* 940-944, 1979.

Korolev A. V., J. W. Strapp, and G. A. Isaac, 1998: Evaluation of accuracy of PMS Optical Array Probes. *J. Atmos. Oceanic Techn.*, **15**, 708-720.

Korolev A. V., J. W. Strapp, and G. A. Isaac, A. N. Nevzorov, 1999: In situ measurements of effective diameter and effective droplet number concentration. *J.Geoph.Res.*, **27**, 3993-4003.

Korolev, A.V., G. Isaac, I. Mazin and H. Barker, 2001: Microphysical properties of continental stratiform clouds. *Quart. J. Roy. Meteor. Soc.,* **127**, 2117-2151

Kosarev, A. L., I. P. Mazin, A. N. Nevzorov, and V. F. Shugaev, 1976: Optical density of clouds. *Trans. Cent. Aerol. Obs.*, *124,* 44-110.

Mazin, I.P., A.V. Korolev, A. Heymsfield, G.A. Isaac, S.G. Cober, 2001: Thermodynamics of Icing Cylinder for Measurements of Liquid Water Content in Supercooled Clouds. *J. Atmos. Oceanic Techn.,* **18**, 543–558

Nevzorov A. N., and V. F. Shugaev, 1974: Aircraft cloud extinction meter. *Trans. of Cent. Aerol. Obs.*, **106,** 3-10.

Nevzorov A. N., and V. F. Shugaev, 1972: The use of integral parameters for study

of cloud microstructure (in Russian), *Trans. Cent. Aerol. Obs.*, *101***,** 32-47.

Ruskin, R.R., 1974: The measurements of cloud elements: the use of transmission and scattering techniques to measure ice and water. *Proc. Symp. Measuremen of Cloud Elements*, W.D. Scott, Ed. NOAA, Tech Memo ERL WMPO-19, 117

Zabrodsky, G.M., 1957: Measurements and some results of study of visibility in clouds. in "*Study of clouds, precipitation and cloud electrification*" Gidrometeizdat, 131-134.

Zmarzly, P.M. and R.P. Lawson, 2000: An Optical Extinctiometer for Cloud Radiation Measurements and Planetary Exploration. Final Report submitted to NASA Goddard Space Flight Center in fulfillment of Contract NAS5-98032, September, 2000, 131 pp. (available from http://www.specinc.com/publications/Extinctiometer_Report.pdf)

Weickmann, H. K. and H. J. aufm Kampe, 1953: Physical properties of cumulus clouds. *J. Atmos. Sci.,* **10**, 204-211